

A Comparative Study on the Roles of Velocity in the Material Removal Rate during Chemical Mechanical Polishing

Wei-Tsu Tseng,^{a,*} Jyh-Hwa Chin,^b Lee-Chieh Kang^b

^aDepartment of Materials Science and Engineering, National Cheng-Kung University, Tainan 701, Taiwan

^bInstitute of Mechanical Engineering, National Chiao-Tung University, Hsinchu 300, Taiwan

Relative velocities between the flowing slurry and selected points on a 150 mm wafer and nonuniformity of velocity are calculated given the known carrier speed, platen speed, and pad-to-wafer distance. Based on simulation results, the combination of a high pad rpm, a medium wafer rpm, and a large pad-to-wafer distance should give rise to a minimum nonuniformity of velocity. Chemical mechanical polish (CMP) removal rates data are fitted to the original Preston equation, Tseng's model,¹ and a modified Preston equation which incorporates the deterioration characteristics of abrasives into the removal rate model. Theoretical removal rate data predicted by Tseng's model and the modified Preston equation exhibit much better agreement with experimental removal rates than those by the original Preston equation. The nonlinear dependence of removal rate on velocity can be explained by the deterioration in slurry abrasion capability.

© 1999 The Electrochemical Society. S0013-4651(97)11-028-X. All rights reserved.

Manuscript submitted November 12, 1997; revised manuscript received February 4, 1999.

Chemical mechanical planarization (CMP) has been widely recognized as the most promising technology to eliminate topographic variation and achieve wafer-level (global) planarization for ultra-large-scale integrated (ULSI) circuits.²⁻³ Despite its extensive utilization, however, the process control of CMP remains at an empirical stage and most users still refer to the Preston equation⁴ as the wafer-scale material removal model. This equation states that the removal rate, RR , is proportional to the product of the polish pressure, P , and velocity, V , i.e.

$$RR = k_p PV \quad [1]$$

where k_p is the Preston coefficient.

Originally proposed for glass polishing, the Preston equation is also of an empirical nature and lacks scientific basis. Uncertainty remains regarding the basic polish behavior. Recent theoretical work and experimental evidence suggest that the Preston equation may overestimate the CMP removal rate.^{1,5} Tseng and Wang¹ proposed an analytical model that predicts a $P^{5/6}V^{1/2}$, instead of Preston's PV dependence of CMP removal rate

$$RR = MP^{5/6}V^{1/2} \quad [2]$$

where M is the weighting factor to removal rate from other processes (e.g., slurry attack). Ouma et al.⁶ observed that, depending on the magnitude of the product of pressure and velocity, there exist two regimes of polish operation so that the addition of a constant term to the Preston equation yields a better fit to experimental results. Similar results have been reported elsewhere.⁷ Overall, the feasibility of Preston equation in describing the CMP removal rate has been challenged and deserves careful and systematic investigation.

Another dilemma associated with the Preston equation is that the definition of V appears vague, since, in an orbital CMP system, the carrier and pad rotate at their respective speeds and the velocity varies from wafer center to edge during polishing. Such a speed variation has been widely observed by most CMP users, and at least two previous studies^{6,8} have analyzed and correlated it with other machine parameters and the polish rate. The clarification of the dependence of pressure and velocity on removal rate would be essential to the CMP process control, since, for example, simulation and prediction of topographic evolution or planarization efficiency depends strongly upon an accurate removal rate model incorporating P and V .

In this work, efforts will be attempted first to reexamine the definition and variation of velocity across a 150 mm wafer during CMP process. Simulation works will follow to investigate the impacts of

velocity variation on polish rate, based on the original Preston equation, Tseng's model,¹ and a modified Preston equation which takes into account the deterioration in the abrasion efficiency of slurry. Comparisons (curve fitting) will be made between experimental polish data and the simulated results based on the three models. The pressure dependence of the removal rate models and other parameters (e.g., weighting factor) are evaluated. The feasibility of the three models is discussed.

Velocity Simulation

In this study, velocity is defined as the relative velocity (v) between an abrasive particle and a specific point on the wafer, during CMP operation. Several assumptions regarding the movement of wafers and abrasive particles need to be established. First, particles are all embedded in the surface features of pad. In this case, the asperity contact model⁹ is adopted. In this model, particles retained on the asperity of pad carry out the abrasion action. This suggests that the maximum abrasion capability of particles occurs when particles are embedded on the asperity of pad. Under this circumstance, the velocity of particles is the same as that of the pad. Second, we assume that no slipping and sliding movement occurs between the wafer and carrier during polishing so that the wafer speed is the same as the carrier speed. In addition, the wafer center coincides with the carrier center.

All geometric and machine parameters are constructed based on an IPEC 372M CMP system for 150 mm wafers. Given known pad revolutions per minute (rpm) (ω_p), wafer rpm (ω_a), and the distance between pad center and wafer center (d), the relative velocity (v) on any specified point on the wafer can be deduced, using the procedure described in the Appendix.

Relative velocities are calculated along the radial direction of a wafer at 13 equally spaced points. From the formulation for v (Eq. A-6 in the Appendix), the relative velocity is found to be a quasi-sinusoidal function of time except at wafer center. The mean velocity \bar{v}_i at a given point i , is defined as

$$\bar{v}_i \equiv \frac{1}{T} \int_0^T v_i(t) dt \quad [3]$$

where T is the total polish time. The nonuniformity of velocity (NUV) can thus be defined as

$$\text{NUV} \equiv (1/\bar{v}) [1/n \sum_{i=1}^n (\bar{v}_i - \bar{v})^2]^{1/2}; \text{ and } \bar{v} \equiv (1/n) \sum_{i=1}^n \bar{v}_i \quad [4]$$

where \bar{v}_i is the mean velocity over total polish time T at a given point i along the wafer radius, r ; and \bar{v} is the average value of mean veloc-

* Electrochemical Society Active Member.

^z E-mail: wtsen@mail.ncku.edu.tw

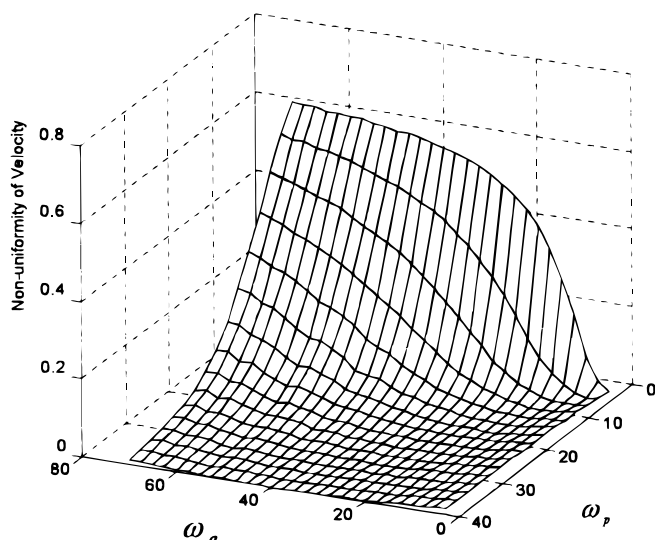


Figure 1. The correlation between NUV, ω_a , and ω_p . The distance between wafer and pad centers, d , is set at 150 mm.

ity over n ($n = 13$) points. The nonuniformity of velocity defined in Eq. 4 represents the degree of variation in the average velocity, \bar{v}_i along the radius of a wafer. The difference in the average velocity between wafer center and edge can enlarge the degree of nonuniformity of velocity. In case \bar{v}_i all over a wafer are exactly the same, the NUV diminishes and the traces of abrasive particles are the same across the wafer.

The nonuniformity of relative velocity across a wafer is plotted against carrier (ω_a) and platen (ω_p) rpms in Fig. 1 for $d = 15$ cm. The result indicates that NUV can be minimized by applying a low carrier speed and a high platen speed simultaneously. Setting a greater d also helps reduce NUV as can be seen in Fig. 2 and 3. Comparison of Fig. 2 and 3 also suggests that (ω_p) has a more pronounced effect on NUV than does (ω_a). On the other hand, NUV remains low over wide ranges of ω_a and d , but increases abruptly at both low and high carrier speeds, as shown in Fig. 3. The above finding that ω_p is more influential than ω_a in determining NUV has also been reported in at least one previous study.⁹

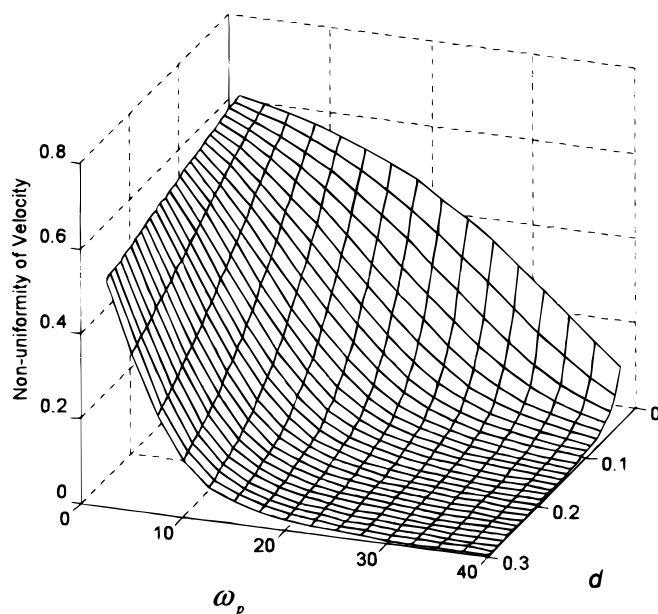


Figure 2. NUV vs. ω_p and d . $\omega_a = 60$ rpm.

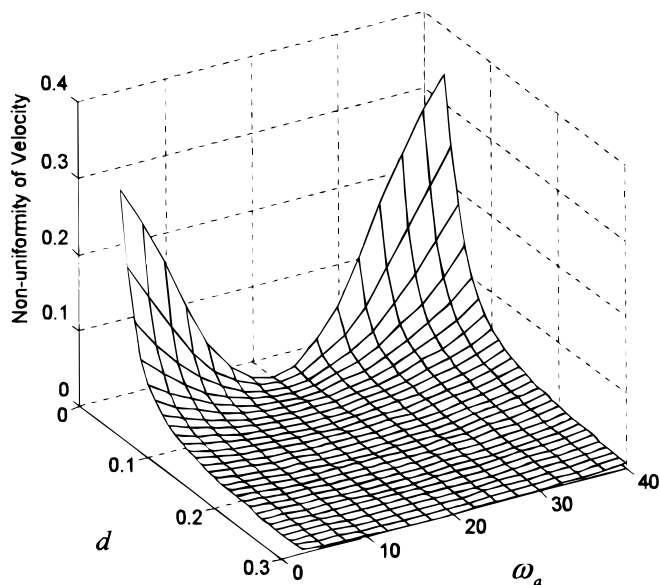


Figure 3. NUV vs. ω_a and d . $\omega_p = 20$ rpm.

Note that the NUV considered herein may not necessarily correspond to the nonuniformity of removal rate, since the latter is a much more complex function of many other factors. Wafer warpage, back pressure, the type of carrier design, pad surface feature, and slurry hydrodynamics, to name a few, all affect removal rate uniformity to certain extent.

To compare the calculated NUV with within-wafer polish non-uniformity (WIWNU), polish experiments were performed on a 1 μ m thick thermal oxide grown on 150 mm wafers. The WIWNU presented here was defined similarly as in Eq. 4 averaged over those obtained from five wafers. On each wafer, removal rates were measured at 49 points evenly across the wafer. A 5 mm edge exclusion was applied to the determination of both NUV and WIWNU. The NUV and WIWNU thus calculated are plotted against pad rpm in Fig. 4 under default conditions of $\omega_a = 42$ rpm, $d = 15$ cm, $P = 7$ psi and back pressure = 2 psi. Although no one-to-one match exists between NUV and WIWNU, the trend is clear. WIWNU decreases as NUV decreases. At low ω_p , the larger relative velocity at wafer edge may have been offset by, for example, the wafer bow effect, leading to a higher pressure at the center and the resulting lower WIWNU than NUV. At high ω_p , on the other hand, uneven slurry abrasive particle distribution and the persisting wafer bow effect may have contributed to the higher-than-expected WIWNU, despite the minimal difference in relative velocity between the wafer center and the edge.

Modak et al.¹⁰ evaluated removal rate and its nonuniformity as a function of the carrier-to-pad rpm ratio (ω_a/ω_p). Their findings indicated that the increase of the ω_a/ω_p ratio over ~ 1.14 resulted in a remarkable increase in WIWNU. In the current study, the NUV data in Fig. 1 and 2, and the WIWNU data in Fig. 4 all exhibit a similar trend. Another important factor to consider is the distance, d , between the wafer center and the pad center. Based on the simulation results in Fig. 2 and 3, the combination of a high pad rpm, a medium wafer rpm, and a large pad-to-wafer distance should give rise to a minimum nonuniformity of velocity. Overall, the findings from the above simulation can serve as general guidelines for improving removal rate uniformity under a well controlled polish condition.

The $V^{1/2}$ dependence of removal rate in Eq. 2 has been verified experimentally.¹ However, in that study, the V term was meant to represent carrier rpm. Thus, the observation that platen is more influential than carrier on the velocity nonuniformity renders it necessary to further clarify the correlation between the V and the RR , based on a more precise definition of velocity. Since velocity actually varies from point to point on a wafer, relative velocity between abrasive

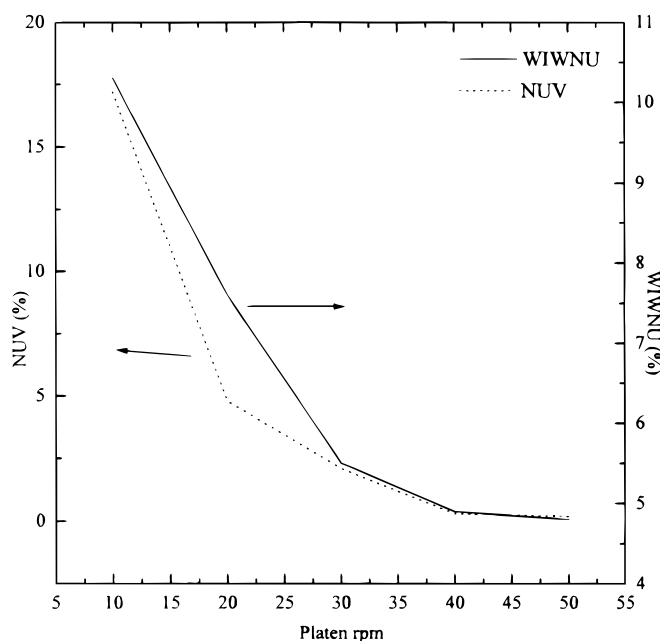


Figure 4. NUV and WIWNU as a function of ω_p . $\omega_a = 42$ rpm; $d = 150$ mm.

particles and a specific point (e.g., wafer center) on the wafer is used in order to truly reflect the removal rate variation.

Degradation of Abrasives during Polishing

Down pressure and velocity are the two most influential process parameters in determining CMP polish characteristics. So far, most of the removal rate models consider pressure and velocity as the most important attributes to removal rate. The role of pressure has been perceived as to force the indenters (abrasives) into the wafer surface.¹¹ On the other hand, velocity represents the shearing rate of the abrasives that plow across the wafer surface, and the rate at which the polish residues get transported away by the flowing slurry.¹² Deviation of removal rate from linear behavior with both pressure and velocity has been observed, and a $P^{5/6}v^{1/2}$ dependence of removal rate is suggested, as mentioned previously.

From another perspective, the deviation of removal rate from linear behavior can be perceived alternatively as the reduction in the number of, or the gradual degradation in the shearing capability of, effective abrasive particles. Mulhearn and Samuels¹³ introduced the concept of fractional available cutting points, f_n , and related it to the removed mass in the formulation of an abrasive machining model. In order to reflect the true abrasive characteristics, the deterioration of abrasion capability should be considered. Abrasives may be worn out gradually during repeated traverses, resulting in deterioration of polishing efficiency.

In a recent study, Zhong and Yang reported that particle aggregation on the pad surface is directly responsible for removal rate decay.¹⁴ It was experimentally verified that the aggregated slurry abrasive particles filled up the pores on pad surface, resulting in the deterioration in abrasion capability.

On both accounts, such a deterioration behavior can be described in form of exponential decay

$$f_n = f_0 \cdot e^{-\alpha n} \quad [5]$$

where f_0 is the fraction of effective abrasion points in an unused slurry, α is the degradation coefficient, and n is the number of traverses. This deterioration phenomenon can not be underrated in a CMP polish model. At the wafer edge where the slurry is fed freshly to the pad/wafer interface, the abrasives would have high abrasion capability. As the slurry flows toward the wafer center, the particles are more likely to aggregate, reducing their abrasion capability and mean velocity. In addition, the longer the particles travel per unit time (i.e.,

high relative velocity), the more likely they would deteriorate or aggregate. Based on the above arguments, a factor of deterioration in the shearing efficiency, f_d , can be introduced in a form similar to f_n

$$f_d = e^{-\beta v} \quad [6]$$

Combining Eq. 1 and 6 yields

$$RR = k_c P (e^{-\beta v}) \quad [7]$$

where k_c is a weighting factor to removal rate, and β is the deterioration coefficient that signifies the degree of particle aggregation and abrasion degradation. Equation 7 can be perceived as a modification to Preston equation in that it incorporates the deterioration characteristics of abrasives into polish behavior.

Comparison Between Removal Rate Models

Equations 1, 2, and 7 represent three CMP removal rate models based on different mechanisms. Simulation of removal rates based on the three models above with the relative velocity was performed at the wafer center (point A), halfway between the wafer center and edge (point B), and the wafer edge (point C, 75 mm away from wafer center), using MATLAB software. All machine parameters were based on a Westech 372M CMP system for 150 mm wafers. To verify the feasibility of the three models, CMP experiments were conducted with 1 μ m thick thermal oxide wafers. The following machine parameters were used for polish experiments: $d = 180$ mm, $\omega_a = 42$ rpm, $\omega_p = 10$ -50 rpm. During experiments, the pressure, P was varied from 4 to 9 psi in order to examine the intercorrelation between pressure and relative velocity, and its effects on removal rate. The pad rpm and its corresponding relative velocity at points A, B, and C are listed in Table I for comparison.

Theoretical removal rates at point A are plotted against the relative velocity, based on the original Preston equation (Eq. 1), Tseng's model (Eq. 2), and the modified Preston equation (Eq. 7) in Fig. 5, 6, and 7, respectively. A cost function, Co , which is an optimization method, is defined in order to calculate the weighting factors (k_p , M , and k_c)

$$Co = (1/m) \sum_{j=1}^m [RR(v_j) - RR_c(v_j)]^2 \quad [8]$$

where m is the number of experimental (velocity) conditions, $RR(v_j)$ is the calculated removal rate based on the model under consideration, and $RR_c(v_j)$ is the experimental removal rate. The cost function can also be used to evaluate the match between experimental data and theoretical prediction by introducing the average value of cost, \bar{C}_o

$$\bar{C}_o = (1/w) \sum C_{oq} \quad (q = 4-9) \quad [9]$$

where $w = 6$ is the number of pressure condition. \bar{C}_o represents the average degree of fit for the six curves under different pressures, based on the specific model under consideration.

The \bar{C}_o values for all three models are shown in Fig. 8, which indicates clearly that Tseng's model and the modified Preston equation proposed in the present study exhibit a much better match with

Table I. Conversion of ω_p into relative velocity at the wafer center (point A), halfway between center and edge (point B) and wafer edge (point C). The ω_a is fixed at 42 rpm. The distance between wafer and pad centers, d , is set at 180 mm.

Platen speed (rpm)	Velocity (m/s)		
	A	B	C
10	0.1900	0.2040	0.2660
20	0.3800	0.3834	0.3960
30	0.5700	0.5708	0.5733
40	0.7600	0.7601	0.7601
50	0.9500	0.9501	0.9507

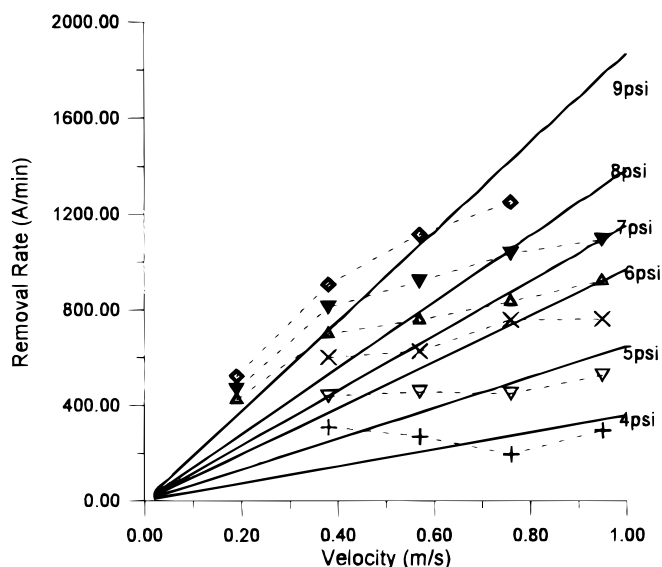


Figure 5. Curve fitting between experimental (dashed) and theoretical (solid) removal rates based on the original Preston equation in Eq. 1.

the experimental results than the original Preston equation. This trend is even more distinct at high pressures as the \bar{C}_o values for Preston equation increase dramatically with increasing pressure. Conversely, for the other two models, the average value of cost is virtually independent of the applied pressure. Since all three models prescribe the similar pressure dependence of removal rate, the large \bar{C}_o values of the original Preston equation, i.e., the large fitting error, would very likely be the consequence of the inadequate velocity term in Eq. 1.

The same procedure is repeated for points B and C. The calculated average value of cost at the three wafer locations for the three models are summarized in Table II. Again, the modified Preston equation exhibits the lowest \bar{C}_o values, suggesting the best fit with experimental data. Tseng's polish rate model also gives low cost values. The original Preston equation, on the other hand, yields \bar{C}_o values that are one order of magnitude higher than the previous two models. Note that, among the three removal rate models considered, only Tseng's model predicts a $P^{5/6}$ dependence of removal rate as described in Eq. 2. This may be the potential source of greater fitting error associated with Tseng's model, relative to the modified Preston

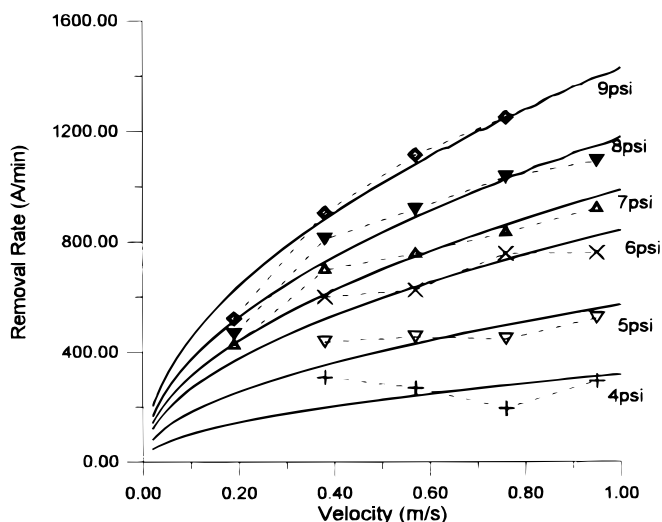


Figure 6. Curve fitting between experimental (dashed) and theoretical (solid) removal rates based on the Tseng's model in Eq. 2.

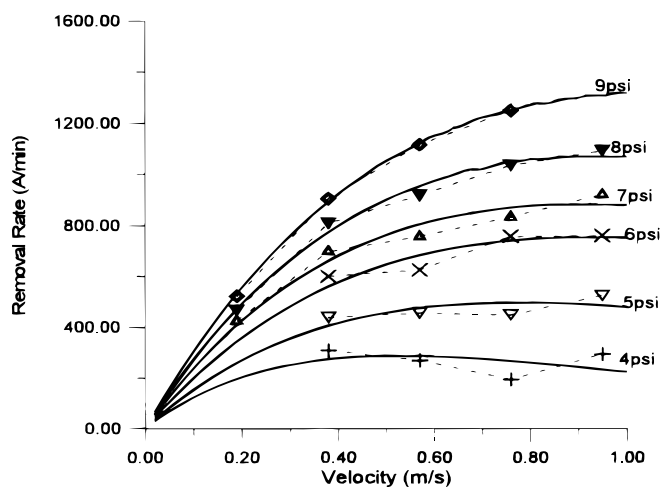


Figure 7. Curve fitting between experimental (dashed) and theoretical (solid) removal rates based on the modified Preston equation in Eq. 7.

equation. Since the difference is slim and the fitting error (i.e., \bar{C}_o) does not widen with increasing pressure as Fig. 8 indicates, we believe that the difference in velocity term is the main attribute to the variation in \bar{C}_o among the three models. However, whether the removal rate does exhibit a linear dependence on pressure deserves further theoretical as well as experimental work to verify it.

Note in Table II that at the wafer edge (point C) where the edge effect¹⁴ occurs, the Preston equation exhibits the poorest fit relative to points A and B, while the other two models seem unaffected by this effect. This may not be attributed to the pressure distribution at the edge as one study pointed out,¹⁵ since both the original and the modified Preston equations prescribe the same functional dependence of removal rate on pressure. Instead, it would most likely result from the relative velocity and slurry flow characteristics on the edge, in the way described in Eq. 2 and 7. This point is elaborated later.

The deterioration coefficient.—The calculated β values are displayed in Fig. 9a-c for points A-C. β is virtually a constant (1.01) at the wafer edge over the pressure range studied. It increases gradually and exhibits greater variation (up to 35%) as the point moves toward the wafer center. The mean β values at points A and C differ by 47%. For comparison, in a separate polish experiment with $d = 10.0$ cm, the mean β values differ by 69% between the wafer center

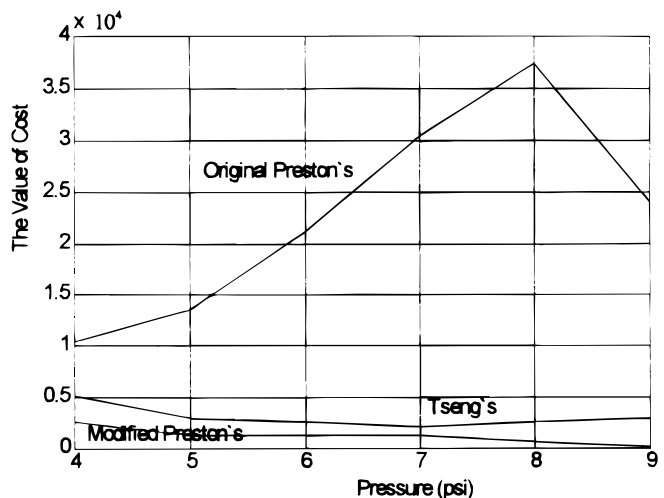


Figure 8. The calculated values of cost, \bar{C}_o , for the three models as a function of pressure at wafer center.

Table II. The average value of cost, \bar{C}_0 , for the three models calculated at the three wafer locations.

	A	B	C
The modified Preston equation	1225	876	986
Tseng's model	3069	2726	1605
The original Preston equation	22839	26095	32753

and edge. The fact that the deterioration coefficient is greater at the wafer center than at the edge seems to support our postulation that the particles are more likely to aggregate at the wafer center.

Interestingly, at point A (wafer center), the deterioration coefficient, β , is greater under lower pressures. Though to a lesser degree, the same trend also occurs at point B. At wafer edge (point C), β varies in a range within the standard deviation (~ 0.29) and is considered a constant. Such a pressure dependence seems contradictory to our intuition, since, under a greater down force, an accelerated polish rate, and hence, faster abrasive degradation would be expected. It is possible that the slurry flow at the wafer center is more random and less regulated under a lower pressure, due to, for example, wafer warpage and insufficient back pressure. As a consequence, the abrasion action is retarded, giving rise to a higher deterioration coefficient. An indirect support for this point is the higher \bar{C}_0 values (greater deviation between experiment and simulation) at the wafer center, as shown in Table II.

The weighting factors.—The calculated k_p , M , and k_c factors for the three models over the pressure range investigated are shown in Fig. 10a, b, and c, respectively, for wafer points A, B, and C. All three weighting factors are highest in magnitude at the wafer edge

and decrease gradually toward wafer center. In terms of pressure dependence, both k_p and M increase with increasing applied pressure and the trend is more pronounced at wafer center than wafer edge. Conversely, the k_c factor for the modified Preston equation remains virtually unchanged over the pressure range, regardless of the wafer position. In Eq. 2, the increase in M with increasing pressure has been found previously.¹ This was attributed to the stress-assisted erosive or corrosive attack by the slurry. In fact, the M factor was perceived to be a function of P and V and its magnitude depends on the pressure range imposed. The k_p factor in the original Preston equation carries the same physical sense as M . As to the modified Preston equation, the chemical component of removal rate may have been accounted for in the deterioration coefficient, β , so that the k_c factor is insensitive to the stress (or pressure) assisted chemical processes. It may only depend on the consumables (e.g., pad) used. If this were the case, the deterioration coefficient, β , would represent not only the decay of abrasion efficiency but also the decline in chemical reaction rate with time during polishing.

The positional variation of weighting factor is somewhat difficult to justify. It could not be the result of wafer warpage and uneven slurry flow, since all three models are equally prone to these effects. It implies that the chemical erosion rate is slightly more intensive at the wafer edge than at its center, while the reverse is true for its pressure dependence. More work related to the fluid behavior is needed to clarify this point.

Pad speed vs. relative velocity.—To evaluate and compare the role of pad speed in the three models with regard to the relative velocity, simulation and curve fitting are repeated for the three models with the V term replaced by ω_p , the pad rpm. The value of cost for the three models calculated at wafer center in this case is plotted against pressure in Fig. 11. Similar to the results in Fig. 8 and Table II, the original Preston equation yields \bar{C}_0 values that are one order of magni-

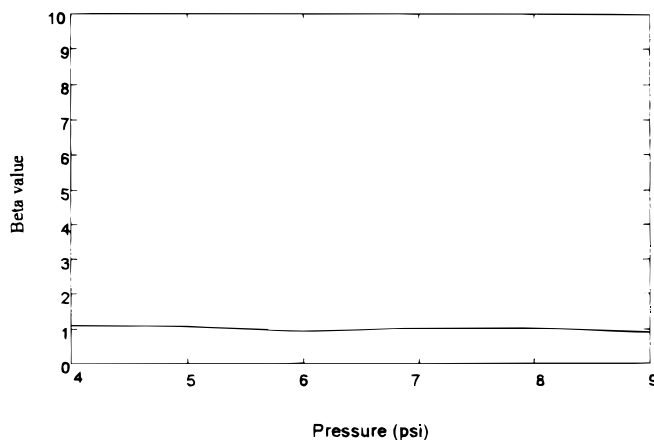
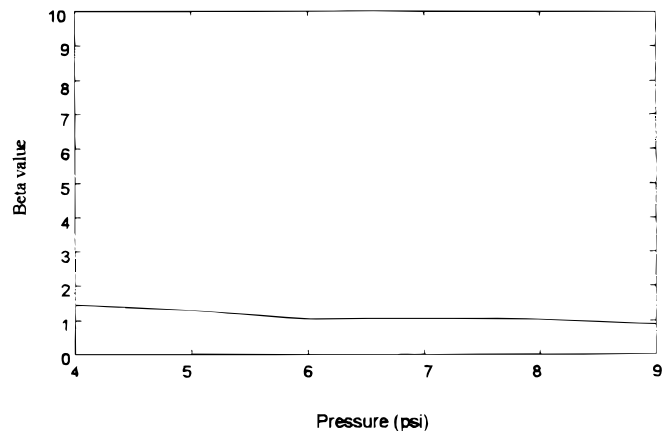
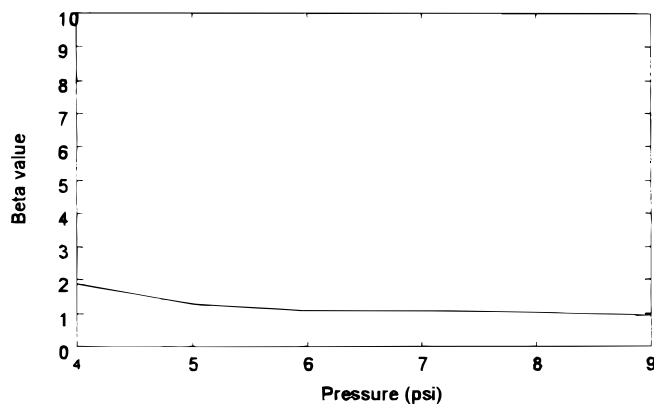


Figure 9. The calculated deterioration coefficient, β , as a function of pressure at (a, top left) wafer center; (b, above) halfway between wafer center and edge; and (c, left) wafer edge.

tude higher than for the other two models. The calculated weighting factors are shown in Fig. 12 for the three models. Again, the trend is similar to that displayed in Fig. 10. The M factor in Tseng's model is

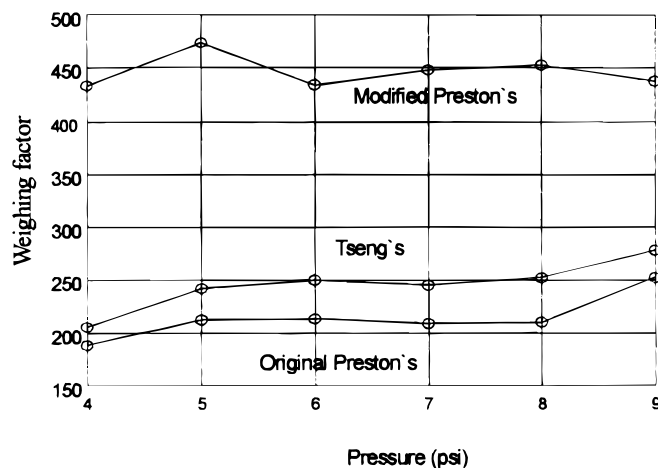
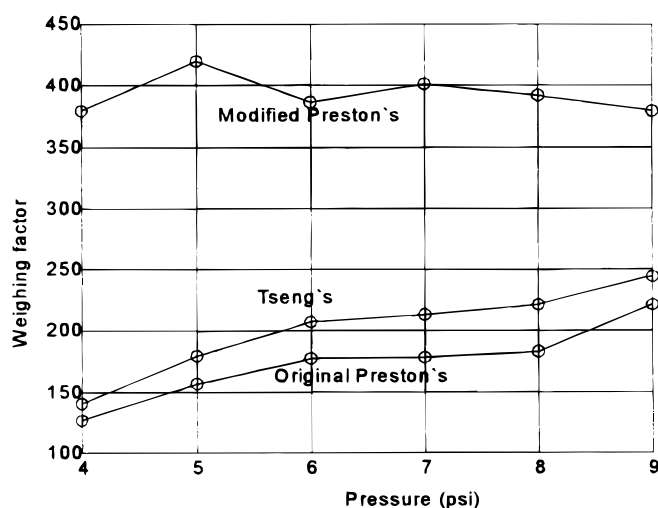
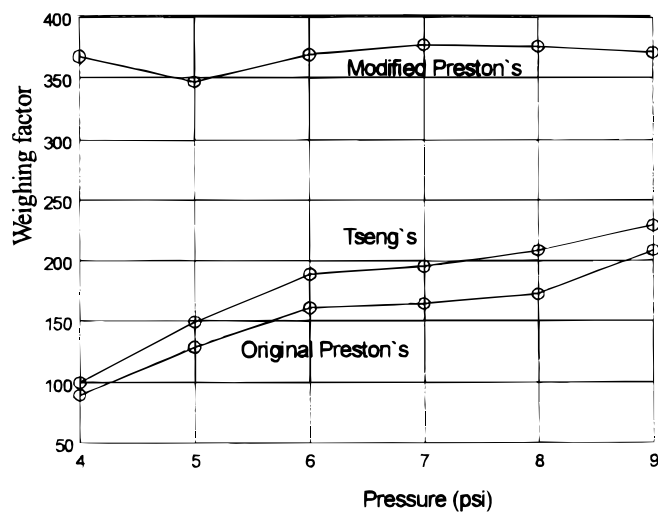


Figure 10. The calculated weighing factors, k_p , M , k_c , respectively, for the original Preston equation, the Tseng's model, and the modified Preston equation vs. pressure at (a) wafer center; (b) halfway between wafer center and edge; and (c) wafer edge.

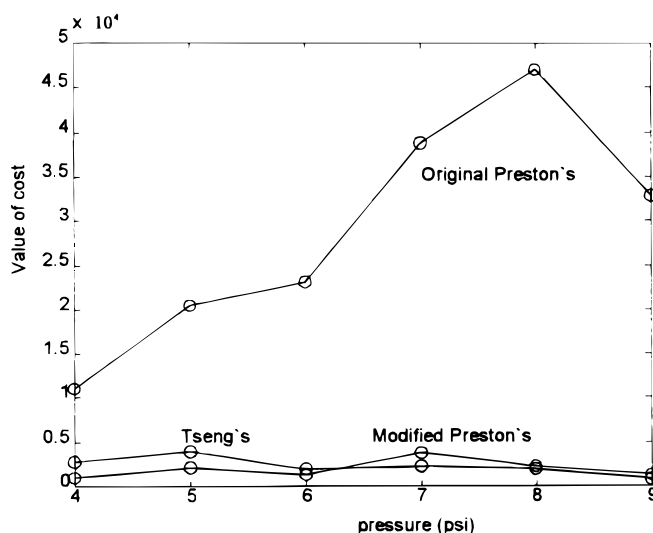


Figure 11. The calculated values of cost, \bar{C}_o , for the three models as a function of pressure at wafer center. The velocity is defined ω_p .

a pressure-dependent quantity, while the k_p and k_c factors for the original and modified Preston equations, respectively, remain virtually unchanged over the pressure range investigated.

Discussion

The low average values of cost of Eq. 7 justify the feasibility of this newly modified removal rate model. Tseng's model also exhibits a good match with experimental data. Relatively speaking, the Preston equation is inaccurate in predicting the CMP removal rate as a function of pressure and velocity. The deterioration in the cutting efficiency of abrasives or the deceleration of chemical reaction rate may explain the saturation of removal rate with increasing velocity. Such a polish behavior is obeyed more faithfully at the wafer edge than at the wafer center. This may arise from the fact that the abrasive supply and slurry flow are more uniform at the wafer edge than at the wafer center. The insensitivity of Tseng's model and the modified Preston equation to the edge effect (rise in polish rate at the edge) may result from the slurry transport characteristics at the edge. In the Tseng model, the velocity term ($V^{1/2}$) is perceived as the rate at which the polish residues get transported away from the abraded points. In the modified Preston equation, an exponential term is included to characterize the deterioration of abrasives with time

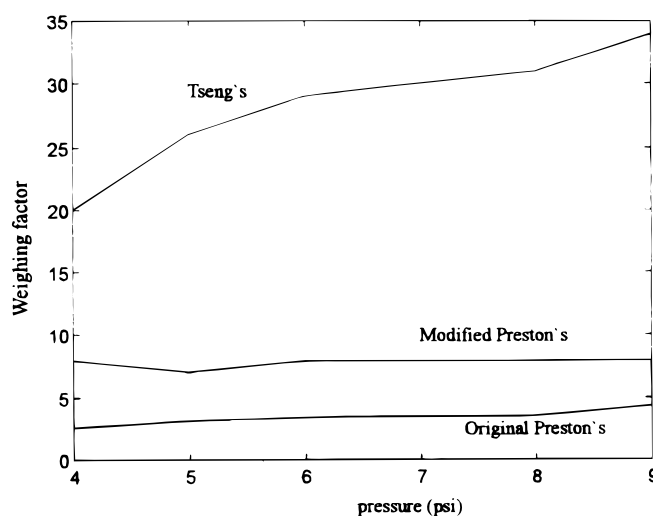


Figure 12. The calculated weighing factors for the three models as a function of pressure. The velocity is defined ω_p .

(velocity). In both cases, relative velocity instead of wafer or pad rpm is used. This relative velocity reflects the trace of a specific point on the wafer, and the "treatment" this point receives along its path. According to Table I, the higher removal rates at the wafer edge (i.e., edge effect) may simply be the direct consequence of the higher relative velocity at the wafer edge, plus the transport processes that the two models depicted above.

This greater variation in β associated with a smaller d ($d = 180$ mm vs. $d = 100$ mm) suggests a greater variation in abrasive deterioration behavior across a wafer, when the distance, d , between carrier center and platen center is reduced. This coincides with the result from the velocity simulation that nonuniformity in velocity increases with decreasing d , and supports the hypothesis that the deterioration coefficient, β , is related directly to the relative velocity.

In Tseng's model, the weighing factor, M , is considered as a variable whose magnitude depends on the values of P and V that are investigated.¹ The same trend is identified in the current study. The original Preston equation, too, exhibits such a phenomenon. However, for the modified Preston equation in Eq. 4, k_c is essentially a constant throughout the pressure and velocity ranges investigated. Based on the data presented in this study, it is still too early to judge if this parameter is a constant or a process-dependent variable. The argument that the β factor may have accounted for the variation in the chemical process requires more experimental evidence to verify it.

The fact that removal rates based on pad speed fit equally well to Tseng's model and the modified Preston equation further demonstrates the feasibility and usefulness of the two models. In addition, it justifies the common belief that pad rpm is more influential on polish behavior. In an orbital CMP system, the relative velocity can be best represented (or approximated) by the pad rpm. However, attention must be paid to the relative size of wafer to pad and the wafer-to-pad distance d . More influence from the ω_a will be felt on the relative velocity as the wafer-to-pad size ratio increases. Also, according to our simulation there is less room for modifying the nonuniformity through the adjustment of d , since d has shrunk in this case.

Still more work is ahead for a robust control of CMP process to be realized. One area of future research is the root of pressure distribution and the effects it would bring about on removal rate and WIWNU. This should include the mechanical interaction between, at least, the pad, the curved wafer (wafer warpage), and the back pressure. Initial results in our lab indicated that calculated pressure profile across the wafer matches closely to the experimental removal rate variation, when fitted to Tseng's model and the modified Preston equation proposed in this study.¹⁶ More experimental work is undergoing to investigate this issue.

Another subject worth pursuing is the behavior of slurry (fluid) under pressure and velocity, and the distribution of the abrasive particles within it. Given the extremely thin layer and, very likely, the multiphase flow nature of the fluid, this task would be quite challenging. Adding to this difficulty is the complex surface feature of pad and how it directs the flow of slurry. Information obtained from the above-mentioned study would reveal more information on the nature of within wafer nonuniformity and help gain more insight into the physical process involved in the characterization of the deterioration coefficient β in this study.

Conclusion

In this study, the kinematics during chemical mechanical polishing are investigated. Nonuniformity of relative velocity is simulated. A greater distance between wafer and pad centers can help reduce velocity nonuniformity. A longer travel distance would result in particle aggregation and degradation of abrasion efficiency, manifested by a saturation of removal rate with increasing velocity. Relative velocity between the wafer and the abrasive is more adequate in describing the removal rate and removal rate nonuniformity during CMP, although pad speed can be used also as an approximation for it in an orbital CMP system. The Preston equation is inadequate in describing the polish rate as a function of velocity. Instead, a modified Preston equation incorporating abrasive deterioration behavior

($e^{-\beta v}$) or a $V^{1/2}$ dependence of removal rate gives better agreement with experimental polish data. The feasibility of these two models seems unaffected by the edge effect.

Acknowledgments

The authors gratefully acknowledge Dr. Wen-Chueh Pan of Chung-Shan Institute of Science and Technology (CSIST) of Lungtan, Taiwan, for his inspiring comments and suggestions throughout the course of the work. This work was supported in part by National Science Council of Taiwan under contract no. NSC 88-2216-E-009-015.

National Cheng-Kung University assisted in meeting the publication costs of this article.

Appendix

The Formulation of Relative Velocity

The geometrical correlation between the pad and carrier during the CMP process is shown in Fig. A-1. The following procedure is used to formulate the relative velocity. From the triangle sine theorem, the relationship between angles θ' and α can be expressed as

$$\frac{r}{\sin \alpha} = \frac{d}{\sin(\theta + \alpha)}$$

or

$$\alpha = \cot^{-1} \left[\frac{\left(\frac{d}{r}\right) - \cos \theta'}{\sin \theta'} \right] \quad [\text{A-1}]$$

where α is the angle between $\overline{O_1P}$ and $\overline{O_2O_1}$, $\theta' =$ the angle between $\overline{O_2O_1}$ and $\overline{O_1P}$, d is the distance between the pad center O_1 and wafer center O_2 , and r is the distance between a designated point P on the wafer and wafer center O_2 .

Applying the triangle sine theorem again, the distance between P and pad center, y , can be solved as

$$\frac{y}{\sin \theta} = \frac{d}{\sin(\theta' + \alpha)}$$

or

$$y = \frac{\sin \theta'}{\sin(\theta' + \alpha)} d \quad [\text{A-2}]$$

Finally, solving for the relative velocity, v ; the velocity of the wafer (V_a), the velocity of the pad (V_p), and the angle between them Φ , can be expressed as

$$V_a = \omega_a r \quad [\text{A-3}]$$

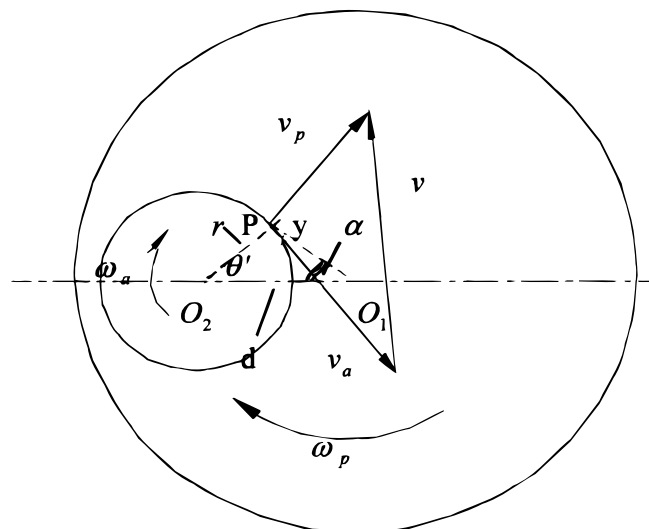


Figure A-1. The schematic showing the relative velocity between wafer and pad.

$$V_p = \omega_p y \quad [\text{A-4}]$$

$$\Phi = \pi - (\theta' + \alpha) \quad [\text{A-5}]$$

from which the absolute value of relative velocity can be formulated

$$|v| = \left\{ |V_p|^2 + |V_a|^2 - 2|V_p||V_a| \cos[\pi - (\theta' + \alpha)] \right\}^{1/2} \quad \text{and } \theta' = \omega_a t \quad [\text{A-6}]$$

where ω_a and ω_p are angular velocities (rpm) of the wafer and pad, respectively, and t is the time elapsed.

References

1. W.-T. Tseng and Y.-L. Wang, *J. Electrochem. Soc.*, **144**, L15 (1997).
2. I. Ali, S. R. Roy, and G. Shinn, *Solid State Technol.*, **37**, 63 (1994).
3. F. Preston, *J. Soc. Glass Technol.*, **11**, 247 (1927).
4. P. H. Singer, *Semicond. Int.*, **15**, 44 (1992).
5. F. Zhang and A. Busnaina, *Electrochem. Solid-State Lett.*, **1**, 184 (1998).
6. D. Ouma, C. Oji, D. Boning, and J. Chung, in *Proceedings of the 3rd International Chemical Mechanical Planarization for ULSI Multilevel Interconnection Conference* (CMP-MIC), p. 20, Santa Clara, CA (1998).
7. Q. Luo, M. A. Fury, and S. V. Babu, in *Proceedings of the 3rd International Chemical Mechanical Planarization for ULSI Multilevel Interconnection Conference* (CMP-MIC), p. 83, Santa Clara, CA (1997).
8. W. T. Tseng, in *Advanced Metallization and Interconnect Systems for ULSI Applications in 1997*, R. Cheung, J. Klein, K. Tsubouchi, M. Murakami, and N. Kobayashi, Editors, p. 617, MRS Conference Proceedings, Materials Research Society, Pittsburgh, PA (1998).
9. T. K. Yu, C. C. Yu, and M. Orłowski, *Tech. Dig. Int. Electron Devices Meet.*, 35.4.1 (1994).
10. A. Modak, P. Monteith, and N. Parekh, in *Proceedings of the 2nd International Chemical Mechanical Planarization for ULSI Multilevel Interconnection Conference* (CMP-MIC), p. 169, Santa Clara, CA (1997).
11. L. Cook, *J. Non-Cryst. Solids*, **120**, 152 (1990).
12. W.-T. Tseng, C.-W. Liu, B.-T. Dai, and C.-F. Yeh, *Thin Solid Films*, **290-291**, 458 (1996).
13. T. O. Mulhearn and L. E. Samuels, *Wear*, **5**, 478 (1962).
14. L. Zhong and J. Yang, in *Chemical Mechanical Planarization*, S. Raghavan, R. L. Opila, and L. Zhang, Editors, PV 98-7, p. 197, The Electrochemical Society Proceedings Series, Pennington, NJ (1998).
15. A. R. Baker, in *Chemical Mechanical Planarization, I*, I. Ali and S. Raghavan, Editors, PV 96-22, p. 228, The Electrochemical Society Proceedings Series, Pennington, NJ (1997).
16. W.-T. Tseng, L.-C. Kang, and W.-C. Pan, in *Proceedings of the 3rd International Chemical Mechanical Planarization for ULSI Multilevel Interconnection Conference* (CMP-MIC), p. 87, Santa Clara, CA (1998).